

# Soft-QCD and UE spectra in pp collisions at very high CM energies (a Snowmass white paper)

Peter Skands

Theory Division, CERN, CH-1211 Geneva 23, Switzerland

(Dated: August 13, 2013)

We make some educated guesses for the extrapolations of typical soft-inclusive (minimum-bias, pileup, underlying-event) observables to proton-proton collisions at center-of-mass energies in the range 13 – 100 TeV. The numbers should be interpreted with (at least) a  $\pm 10\%$  uncertainty.

## I. SOFT PHYSICS MODELS AND ENERGY SCALING

Soft physics models can essentially be divided into two broad categories. The first starts from perturbative QCD (partons, matrix elements, jets) and uses a factorized perturbative expansion for the hardest parton-parton interaction, combined with detailed models of hadronization and (soft and hard) multiparton interactions (MPI). This is the approach taken by general-purpose event generators, like HERWIG [1, 2], PYTHIA [3, 4], and SHERPA [5]. Since they agree with perturbative QCD (pQCD) at high  $p_{\perp}$ , they are used extensively by the collider-physics community, see [6, 7] for reviews. The price is a typically reduced predictivity for very soft physics. Collisions involving nuclei with  $A \geq 2$  are generally not addressed at all by these generators, though extensions exist [8, 9].

At the other end of the spectrum are tools starting from Regge theory (optical theorem, cut and uncut pomerons), like QGSJET [10] and SIBYLL [11]. These are typically used e.g. for cosmic-ray air showers and for heavy-ion collisions. The main focus is here on the soft physics, though perturbative contributions can be added in, e.g. by the introduction of a “hard pomeron”. Inbetween are tools like PHOJET [12], DPMJET [13], and EPOS [14], which contain elements of both languages (with EPOS adding a further component: hydrodynamics [15]). Note, however, that all of these models rely on string models of hadronization and hence have some overlap with PYTHIA on that aspect of the event modeling.

The educated guesses in this summary are based mainly on the energy scaling exhibited by the Perugia 2012 set of tunes [16] of the  $p_{\perp}$ -ordered MPI model [17, 18] in the PYTHIA 6 generator, which have been validated to give an acceptable description of the scaling of a wide range of min-bias and underlying-event observables from lower collider energies to the LHC [16, 19] (see e.g., [mcplots.cern.ch](http://mcplots.cern.ch) [19, 20]). The set also includes several theory uncertainty variations (e.g., of renormalization scales, PDFs, IR cutoffs, and color reconnections). For minimum-bias and pile-up type observables, we also draw on comparisons to EPOS, SIBYLL, and QGSJET, taken from the study in [21].

In MPI-based models, one should be aware that the amount of soft MPI is sensitive to the PDFs at low  $x$  and  $Q^2$ , a region which is not especially well controlled. Physically, color screening and/or saturation effects should be important. In practice, one introduces an  $E_{\text{CM}}$ -dependent regularization scale,  $p_{\perp 0}$ , illustrated for the Perugia models in the left-hand pane of fig. 1. There is then still a dependence on the low- $x$  behavior of the PDF around that scale, illustrated in the right-hand pane. Note the freezing of the PDFs at very low  $x$  (only marginally relevant for  $E_{\text{CM}} \leq 100$  TeV). Note also that NLO PDFs should not be used for MPI models, since they are not probability densities (e.g., they can become negative, illustrated here by the MSTW2008 NLO set [22]). The Perugia 2012 tunes are based on the CTEQ6L1 LO PDF set [23], but include MSTW2008 LO [22] and MRST LO\*\* [24] variations.

The issue of final-state color reconnections (CR) is another important aspect which is less than optimally understood. Physically, this may reflect a generalization of color coherence, and/or dense-packing effects (parton-, string-, or hadron-rescattering). In practice, the Perugia tunes employ a nonperturbative CR model which is based on the string area law [26, 27]. There are indications that higher CM energies may require a smaller effective CR strength [28]. If so, multiplicities could effectively increase a bit faster than we assume here, a possibility we take into account when we evaluate the extrapolation uncertainties.

## II. EXTRAPOLATIONS TO VERY HIGH ENERGIES

For the total cross section, we take a simple Donnachie-Landshoff fit with  $\epsilon \sim 0.08$  [29], which is also the basis of the scaling ansätze made in PYTHIA [30]. As can be seen in fig. 2, ALICE measurements of the inelastic and single-diffractive cross sections [31] exhibit no significant deviations from this ansatz over the measured range. Note that the various diffractive components cannot be unambiguously defined without a specific observable definition (supplied by ALICE as a cut on the mass of the diffractive system,  $M_X < 200$  MeV). The extrapolations yield an inelastic cross section growing from  $\sim 80$  mb at 13 TeV to  $\sim 90$  mb at 30 TeV and  $\sim 105$  mb at 100 TeV, while the elastic cross section (not shown) increases from about 22 mb to 25 mb and 32 mb in the same range. The diffractive components

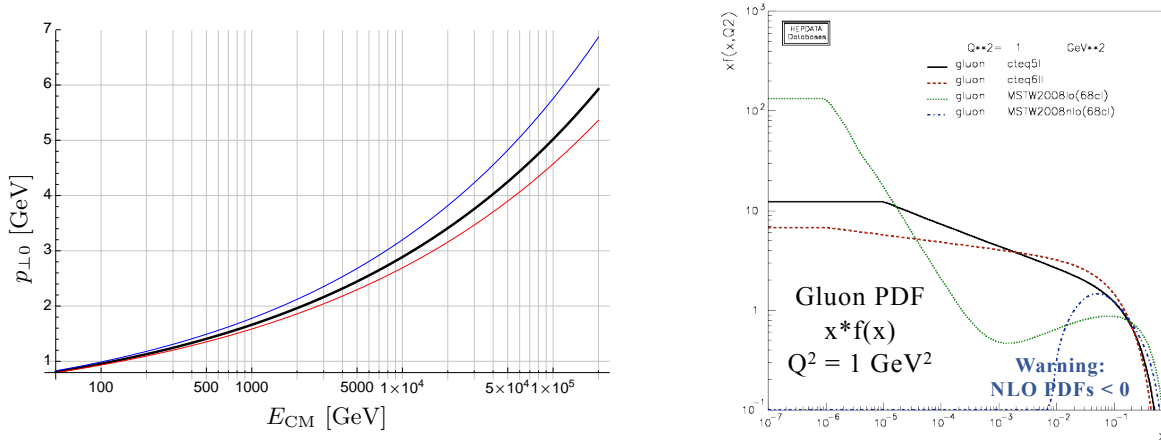


FIG. 1: *Left*: energy scaling of the  $p_{\perp 0}$  soft-MPI regularization scale in the Perugia tunes (central value and range). *Right*: behavior of some typical PDF sets at very low  $Q^2 = 1 \text{ GeV}^2$ , plot from HEPDATA [25].

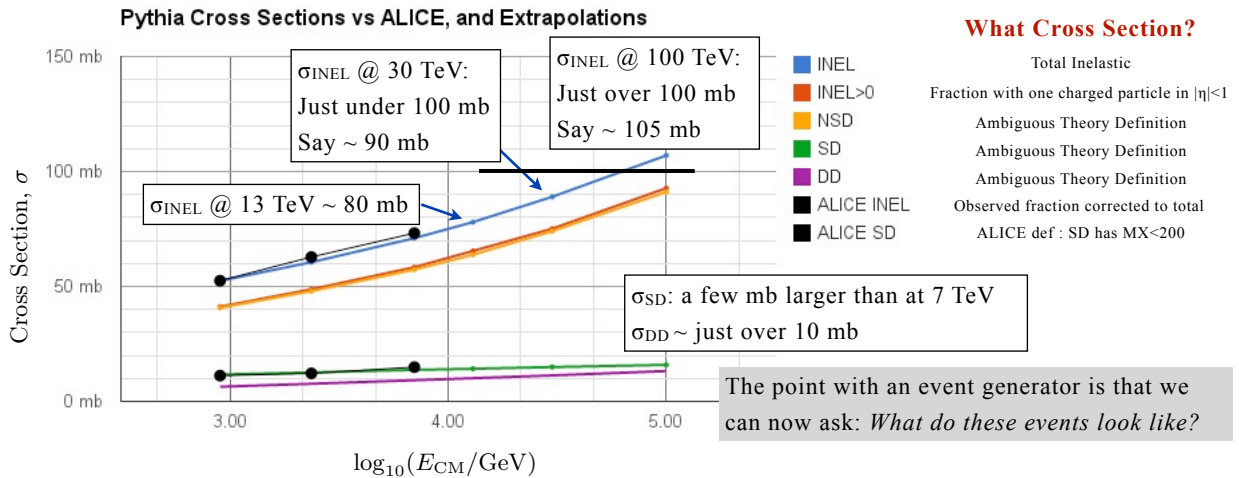


FIG. 2: Assumed scaling of various inelastic components of the total cross section in PYTHIA 6.

increase by only a few mb relative to their 7-TeV values. We can now take a closer look at what these collisions look like. How many tracks, and how much energy deposition are they associated with?

Extrapolations of central charged-track densities in so-called non-single-diffractive events in pomeron-based models are shown in the left-hand pane of fig. 3, from [21]. We note that the version of EPOS used in [21] predicts a much too slow rise with CM energy, while QGSJET II errs severely in the opposite direction, thus we exclude them from our estimates. The PHOJET and PYTHIA generators are represented on the right-hand pane of fig. 3, which contains an update of a highly sensitive plot made by the ALICE collaboration [32, 33]. It shows the relative increase in central charged-track multiplicity between 900 GeV and the 2360 and 7000 GeV CM energies at the LHC, for events with at least one charged track inside  $|\eta| < 1$  (INEL>0). Both PHOJET and the Tevatron tunes of PYTHIA 6 (DW and Perugia 0) exhibit too slow increases with energy, and hence are not included in our extrapolations. The Perugia 2012 and PYTHIA 8 (tune 4C [34]) models, however, manage to reproduce the scaling observed by ALICE fairly well. They can therefore be used as a reasonable first guess for further extrapolations, illustrated in the top pane of fig. 4. Combining the Perugia uncertainty variations with the SIBYLL and QGSJET 01 scaling trends yields an estimated central charged-track density per unit  $\Delta\eta\Delta\phi$  of  $1.1 \pm 0.1$  at 13 TeV,  $1.33 \pm 0.14$  at 30 TeV, and  $1.8 \pm 0.4$  at 100 TeV, for inelastic events with at least one track inside  $|\eta| < 1$  (corresponding to the red cross-section curve in fig. 2).

Note that, when imposing  $p_{\perp}$  cuts on the tracks, one should be aware that indications from the LHC so far are that the  $p_{\perp}$  spectra produced by PYTHIA are slightly too hard [19], with a deficit of about 20% for  $p_{\perp}$  values below  $\sim 200$  MeV, and a similar excess above  $\sim 4$  GeV. (This applies to inclusive charged tracks. Uncertainties are substantially larger for identified particles.) Going from  $|\eta| < 1$  to  $|\eta| \leq 3$ , say, does not change these predictions considerably. There is the trivial seagull-shaped pseudorapidity distribution (roughly a 10% effect), but no other major differences

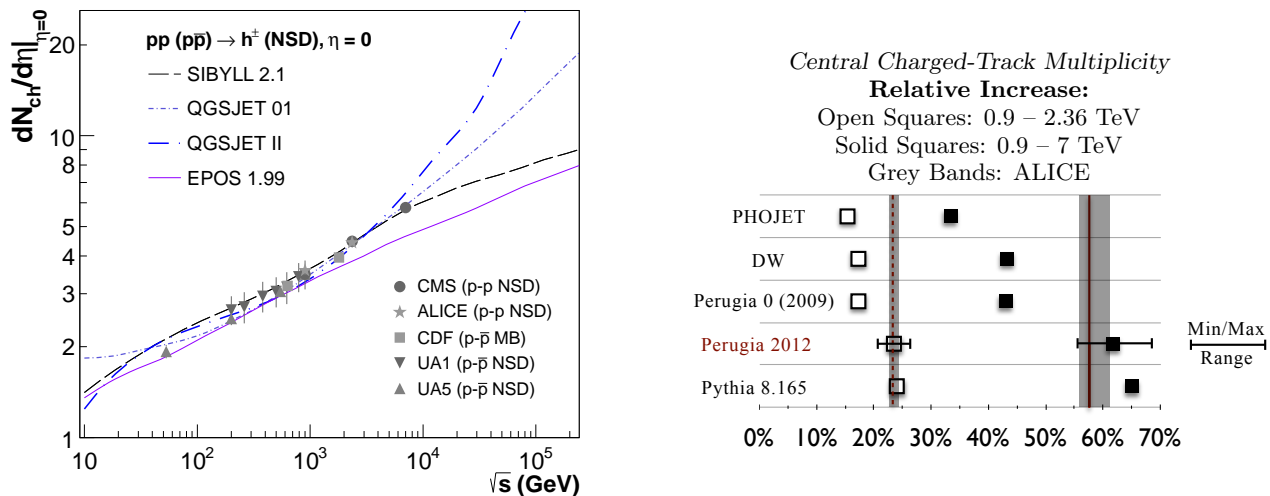


FIG. 3: *Left*: scaling of the central charged multiplicity for SIBYLL, QGSJET, and EPOS, compared with collider data for NSD events, from [21]. *Right*: updated version of a plot in [32] including present-day PYTHIA 6 and 8 tunes.

in estimated track densities or spectra.

An important quantity for jet energy scale calibrations is the amount of transverse energy deposited in the detector, per unit  $\Delta R^2 = \Delta\eta \times \Delta\phi$ , per inelastic collision (corresponding to the blue cross-section curve in fig. 2). In the central region of the detector, the Perugia models are in good agreement with ATLAS measurements at 7 TeV [19, 35], while the activity in the forward region is underestimated [19, 35–37]. Extrapolations lead to an estimated  $1.0 \pm 0.15$  GeV of transverse energy deposited per unit  $\Delta R^2$  in the central region of the detector at 30 TeV, growing to  $1.25 \pm 0.2$  GeV at 30 TeV, and  $1.9 \pm 0.35$  GeV at 100 TeV, shown in the middle pane of fig. 4. We emphasize that similar extrapolations in the forward region would likely result in underestimates by up to a factor 1.5, at least if done with current PYTHIA models.

The last quantity we consider is the activity in the underlying event (UE). The most important UE observable is the summed  $p_{\perp}$  density in the so-called “TRANSVERSE” region, defined as the wedge  $60 - 120^\circ$  away in azimuth from a hard trigger jet. For  $p_{\perp}^{\text{jet}}$  values above 5 – 10 GeV, this distribution is effectively flat, i.e., to first approximation it is independent of the jet  $p_{\perp}$ . It does, however, depend significantly on the CM energy of the pp collision, a feature which places strong constraints on the scaling of the  $p_{\perp 0}$  scale of MPI models, cf. fig. 1. Given the good agreement between the Perugia 2012 models and Tevatron and LHC UE measurements [19], we estimate the  $E_T$  (neutral+charged) density in the TRANSVERSE region (inside  $|\eta| < 2.5$ ), for a reference case of 100-GeV dijets in the bottom pane of fig. 4: starting from an average of about 2.1 GeV per  $\Delta R^2$  at 900 GeV, the density rises to  $3.3 \pm 0.2$  GeV at 13 TeV,  $3.65 \pm 0.25$  GeV at 30 TeV, and  $4.4 \pm 0.45$  GeV at 100 TeV. Note that the charged-only fraction of this would be about a factor 1.6 less.

### Acknowledgments

We are grateful to the volunteers participating in the LHC@home 2.0 project “Test4Theory” [38] for the CPU time they contribute to the `mcplots.cern.ch` web site [19], used in this work. Also many thanks to D. d’Enterria for providing the plot shown in the left-hand pane of fig. 3.

- 
- [1] G. Corcella, I. Knowles, G. Marchesini, S. Moretti, K. Odagiri, *et al.*, “HERWIG 6: An Event generator for hadron emission reactions with interfering gluons (including supersymmetric processes),” *JHEP* **0101** (2001) 010, [hep-ph/0011363](#).
- [2] M. Bähr, S. Gieseke, M. Gigg, D. Grellscheid, K. Hamilton, *et al.*, “Herwig++ Physics and Manual,” *Eur.Phys.J.* **C58** (2008) 639–707, [0803.0883](#).
- [3] T. Sjöstrand, S. Mrenna, and P. Z. Skands, “PYTHIA 6.4 Physics and Manual,” *JHEP* **0605** (2006) 026, [hep-ph/0603175](#).

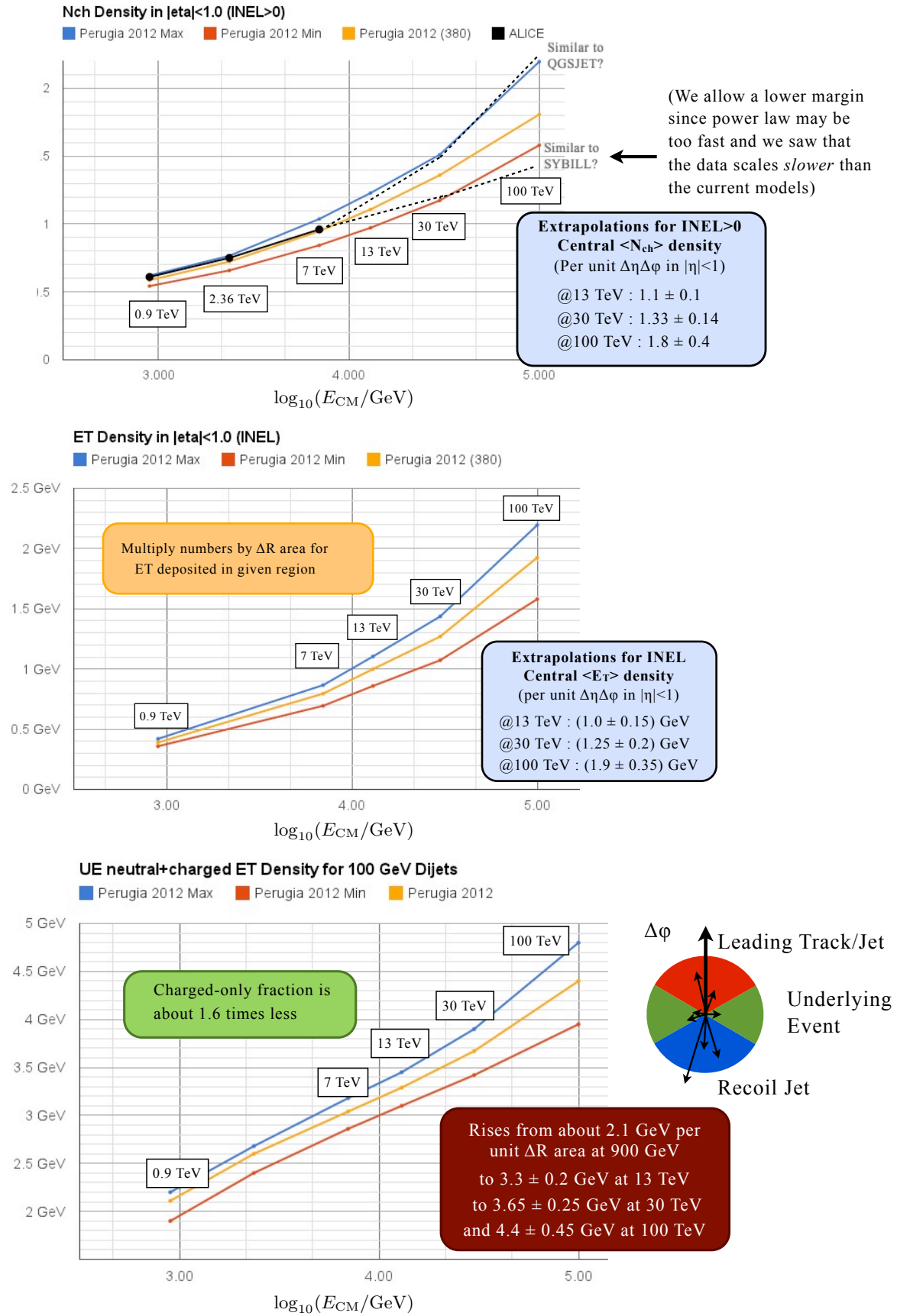


FIG. 4: Extrapolations of the central ( $|\eta| < 1$ ) charged-track density for INEL > 0 events (Top), central ( $|\eta| < 1$ )  $E_T$  density for INEL events (Middle), and central ( $|\eta| < 2.5$ ) UE  $E_T$  density for 100-GeV dijet events (Bottom).

- [4] T. Sjöstrand, S. Mrenna, and P. Z. Skands, “A Brief Introduction to PYTHIA 8.1,” *Comput.Phys.Commun.* **178** (2008) 852–867, 0710.3820.
- [5] T. Gleisberg, S. Höche, F. Krauss, M. Schönherr, S. Schumann, *et al.*, “Event generation with SHERPA 1.1,” *JHEP* **0902** (2009) 007, 0811.4622.
- [6] A. Buckley, J. Butterworth, S. Gieseke, D. Grellscheid, S. Höche, *et al.*, “General-purpose event generators for LHC physics,” *Phys.Rept.* **504** (2011) 145–233, 1101.2599.
- [7] P. Z. Skands, “QCD for Collider Physics,” 1104.2863.
- [8] N. Armesto, L. Cunqueiro, and C. A. Salgado, “Q-PYTHIA: A Medium-modified implementation of final state radiation,” *Eur.Phys.J.* **C63** (2009) 679–690, 0907.1014.
- [9] M. Gyulassy and X.-N. Wang, “HIJING 1.0: A Monte Carlo program for parton and particle production in high-energy hadronic and nuclear collisions,” *Comput.Phys.Commun.* **83** (1994) 307, nucl-th/9502021.
- [10] S. Ostapchenko, “QGSJET-II: Towards reliable description of very high energy hadronic interactions,” *Nucl.Phys.Proc.Suppl.* **151** (2006) 143–146, hep-ph/0412332.
- [11] E.-J. Ahn, R. Engel, T. K. Gaisser, P. Lipari, and T. Stanev, “Cosmic ray interaction event generator SIBYLL 2.1,” *Phys.Rev.* **D80** (2009) 094003, 0906.4113.
- [12] F. W. Bopp, R. Engel, and J. Ranft, “Rapidity gaps and the PHOJET Monte Carlo,” hep-ph/9803437.
- [13] F. W. Bopp, J. Ranft, R. Engel, and S. Roesler, “Antiparticle to Particle Production Ratios in Hadron-Hadron and d-Au Collisions in the DPMJET-III Monte Carlo,” *Phys.Rev.* **C77** (2008) 014904, hep-ph/0505035.
- [14] K. Werner, I. Karpenko, T. Pierog, M. Bleicher, and K. Mikhailov, “Event-by-Event Simulation of the Three-Dimensional Hydrodynamic Evolution from Flux Tube Initial Conditions in Ultrarelativistic Heavy Ion Collisions,” *Phys.Rev.* **C82** (2010) 044904, 1004.0805.
- [15] K. Werner, “Core-corona separation in ultra-relativistic heavy ion collisions,” *Phys.Rev.Lett.* **98** (2007) 152301, 0704.1270.
- [16] P. Z. Skands, “Tuning Monte Carlo Generators: The Perugia Tunes,” *Phys.Rev.* **D82** (2010) 074018, 1005.3457.
- [17] T. Sjöstrand and P. Z. Skands, “Multiple interactions and the structure of beam remnants,” *JHEP* **0403** (2004) 053, hep-ph/0402078.
- [18] T. Sjöstrand and P. Z. Skands, “Transverse-momentum-ordered showers and interleaved multiple interactions,” *Eur.Phys.J.* **C39** (2005) 129–154, hep-ph/0408302.
- [19] A. Karneyeu, L. Mijovic, S. Prestel, and P. Skands, “MCPLOTS: a particle physics resource based on volunteer computing,” 1306.3436. <http://mcplots.cern.ch>.
- [20] A. Buckley, J. Butterworth, L. Lonnblad, H. Hoeth, J. Monk, *et al.*, “Rivet user manual,” 1003.0694.
- [21] D. d’Enterria, R. Engel, T. Pierog, S. Ostapchenko, and K. Werner, “Constraints from the first LHC data on hadronic event generators for ultra-high energy cosmic-ray physics,” *Astropart.Phys.* **35** (2011) 98–113, 1101.5596.
- [22] A. Martin, W. Stirling, R. Thorne, and G. Watt, “Parton distributions for the LHC,” *Eur.Phys.J.* **C63** (2009) 189–285, 0901.0002.
- [23] J. Pumplin, D. Stump, J. Huston, H. Lai, P. M. Nadolsky, *et al.*, “New generation of parton distributions with uncertainties from global QCD analysis,” *JHEP* **0207** (2002) 012, hep-ph/0201195.
- [24] A. Sherstnev and R. Thorne, “Different PDF approximations useful for LO Monte Carlo generators,” 0807.2132.
- [25] A. Buckley and M. Whalley, “HepData reloaded: Reinventing the HEP data archive,” *PoS ACAT2010* (2010) 067, 1006.0517.
- [26] M. Sandhoff and P. Z. Skands, “Colour annealing - a toy model of colour reconnections,” FERMILAB-CONF-05-518-T, in hep-ph/0604120.
- [27] P. Z. Skands and D. Wicke, “Non-perturbative QCD effects and the top mass at the Tevatron,” *Eur.Phys.J.* **C52** (2007) 133–140, hep-ph/0703081.
- [28] H. Schulz and P. Skands, “Energy Scaling of Minimum-Bias Tunes,” *Eur.Phys.J.* **C71** (2011) 1644, 1103.3649.
- [29] A. Donnachie and P. Landshoff, “Total cross-sections,” *Phys.Lett.* **B296** (1992) 227–232, hep-ph/9209205.
- [30] G. A. Schuler and T. Sjöstrand, “Hadronic diffractive cross-sections and the rise of the total cross-section,” *Phys.Rev.* **D49** (1994) 2257–2267.
- [31] ALICE Collaboration, B. Abelev *et al.*, “Measurement of inelastic, single- and double-diffraction cross sections in proton–proton collisions at the LHC with ALICE,” *Eur.Phys.J.* **C73** (2013) 2456, 1208.4968.
- [32] ALICE Collaboration, K. Aamodt *et al.*, “Charged-particle multiplicity measurement in proton-proton collisions at  $\sqrt{s} = 7$  TeV with ALICE at LHC,” *Eur.Phys.J.* **C68** (2010) 345–354, 1004.3514.
- [33] ALICE Collaboration, K. Aamodt *et al.*, “Charged-particle multiplicity measurement in proton-proton collisions at  $\sqrt{s} = 0.9$  and 2.36 TeV with ALICE at LHC,” *Eur.Phys.J.* **C68** (2010) 89–108, 1004.3034.
- [34] R. Corke and T. Sjöstrand, “Interleaved Parton Showers and Tuning Prospects,” *JHEP* **1103** (2011) 032, 1011.1759.
- [35] ATLAS Collaboration, G. Aad *et al.*, “Measurements of the pseudorapidity dependence of the total transverse energy in proton-proton collisions at  $\sqrt{s} = 7$  TeV with ATLAS,” *JHEP* **1211** (2012) 033, 1208.6256.
- [36] CMS Collaboration, S. Chatrchyan *et al.*, “Measurement of energy flow at large pseudorapidities in  $pp$  collisions at  $\sqrt{s} = 0.9$  and 7 TeV,” *JHEP* **1111** (2011) 148, 1110.0211.
- [37] TOTEM Collaboration, G. Antchev *et al.*, “Measurement of the forward charged particle pseudorapidity density in  $pp$  collisions at  $\sqrt{s} = 7$  TeV with the TOTEM experiment,” *Europhys.Lett.* **98** (2012) 31002, 1205.4105.
- [38] D. Lombrana Gonzalez, F. Grey, J. Blomer, P. Buncic, A. Harutyunyan, *et al.*, “Virtual machines & volunteer computing: Experience from LHC@Home: Test4Theory project,” *PoS ISGC2012* (2012) 036.